Epimers of Azaspiracids: Isolation, Structural Elucidation, Relative LC-MS Response, and *In Vitro* Toxicity of 37-*epi*-Azaspiracid-1

Jane Kilcoyne,[†,*] Pearse McCarron,[‡] Michael J. Twiner,[§] Ciara Nulty,[†] Sheila Crain,[‡] Michael A. Quilliam,[‡] Frode Rise,[∥] Alistair L. Wilkins,[⊥,#] and Christopher O. Miles[⊥,○]

[†]Marine Institute, Rinville, Oranmore, Co. Galway, Ireland. Email: jane.kilcoyne@marine.ie

[‡]National Research Council Canada, Measurement Science and Standards, 1411 Oxford Street, Halifax, Nova Scotia, B3H 3Z1, Canada

[§]Department of Natural Sciences, University of Michigan-Dearborn, Dearborn, MI, USA

[∥]Department of Chemistry, University of Oslo, N-0315 Oslo, Norway

[⊥]Norwegian Veterinary Institute, P.O. Box 750 Sentrum, 0106 Oslo, Norway

[#]Department of Chemistry, The University of Waikato, Private Bag 3105, Hamilton, New Zealand

[○]Department of Pharmaceutical Chemistry, School of Pharmacy, University of Oslo, P.O. Box 1068 Blindern, N- 0316 Oslo, Norway

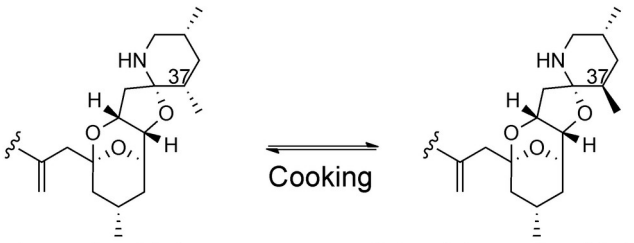

Azaspiracid-1

37-*epi*-Azaspiracid-1
(5-fold more toxic)

ABSTRACT

Since azaspiracid-1 (AZA1) was identified in 1998, the number of AZA analogues has increased to over 30. The development of an LC-MS method using a neutral mobile phase led to the discovery of isomers of AZA1, AZA2 and AZA3, present at ~ 2–16% of the parent analogues in phytoplankton and shellfish samples. Under acidic mobile phase conditions, isomers and their parents are not separated. Stability studies showed that these isomers were spontaneous epimerization products whose formation is accelerated with the application of heat.

The AZA1 isomer was isolated from contaminated shellfish and identified as 37-*epi*-AZA1 by nuclear magnetic resonance (NMR) spectroscopy and chemical analyses. Similar analysis indicated that the isomers of AZA2 and AZA3 corresponded to 37-*epi*-AZA2 and 37-*epi*-AZA3, respectively. The 37-epimers were found to exist in equilibrium with the parent compounds in solution. 37-*epi*-AZA1 was quantitated by NMR and relative molar response studies were performed to determine potential differences in LC-MS response of AZA1 and 37-*epi*-AZA1.

Toxicological effects were determined using Jurkat T lymphocyte cells as an *in vitro* cell model. Cytotoxicity experiments employing a metabolically-based dye (i.e., MTS) indicated that 37-*epi*-AZA1 elicited a lethal response that was both concentration- and time-dependent, with EC_{50} values in the sub-nanomolar range. Based on EC_{50} comparisons, 37-*epi*-AZA1 was 5.1-fold more potent than AZA1. This data suggests the presence of these epimers in seafood products should be considered in the analysis of AZAs for regulatory purposes.

KEYWORDS: azaspiracid, stability, NMR, mass spectrometry, purification, epimerization.

INTRODUCTION

Azaspiracids (AZAs) are marine biotoxins (Figure 1) that originate from the phytoplankton *Azadinium*[1] and *Amphidoma*[2] spp. and that can accumulate in shellfish. The consumption of AZA-contaminated shellfish can lead to a human poisoning called azaspiracid shellfish poisoining.[3] *A. spinosum* has been shown to produce AZA1 and AZA2,[4] while many of the other analogues are produced as a result of metabolism within the shellfish.[5,6] The number of known AZA analogues in this group has increased considerably[7] since they were first discovered in 1998.[3] However, only AZA1, AZA2 and AZA3 are regulated by the EU.[8] To date, only AZA1–6 have been isolated and fully characterized.[3,9–11]

AZAs have been responsible for seven confirmed shellfish poisoning events.[12] Symptoms generally include gastrointestinal illness, such as nausea, vomiting, severe diarrhea, and stomach cramps.[13] In animals, they can elicit similar diarrhetic effects[14] with severe intestinal pathology[15] but extracts given via *i.p*. injection exhibited "neurotoxin-like" symptoms characterized by sluggishness, respiratory difficulties, spasms, progressive paralysis, and death within 20–90 minutes.[16,17] In feeding studies, the AZAs have been shown to be absorbed and systemically distributed with some microscopic pathology associated with the small intestine.[18–20] *In vitro*, the AZAs are also highly cytotoxic to various cell types, with cell death via apoptosis[21] occurring in low nanomolar concentrations.[22–25] Structure–activity relationship studies have shown that there are distinct differences in the potencies of the AZA analogues. AZA2 is the most potent, followed by AZA3, AZA1, and then the hydroxylated AZA4 and AZA5.[9,16,26] The only target conclusively demonstrated for the AZAs has been the hERG potassium channel.[27]

Liquid chromatography–mass spectrometry (LC-MS) is the reference method for the analysis of lipophilic marine biotoxins in shellfish.[8] Considerable efforts were made to produce certified reference materials (CRMs) for AZAs,[28–31] which are now available.[32,33] The availability of CRMs is necessary to ensure accuracy of analytical results. A number of LC-MS methods for the analysis of AZAs have been published employing acidic[34–36] and basic[37] mobile phases. More recently, an LC-MS method for lipophilic toxin analysis was reported that used a neutral mobile phase.[38] This method revealed the presence of unidentified isomers of AZA1, AZA2 and AZA3 in tissue and calibrant CRMs. These isomers were resolved using a neutral eluent but co-eluted with the parent toxin in an acidic eluent.[33] The proportion of

these isomers for AZA1–3 in the tissue CRM ranged from 2–16% of their parent analogues. This finding is significant due to the potential of these isomers to interfere with the accuracy of analytical results. Although these isomers are not typically resolved using acidic and basic[37] methods, they may lead to discrepancies in analytical results depending on the amount present and their relative response factors. Isomers of AZAs have been reported previously but these were produced as a result of acid-catalyzed degradation of the main analogues, and the isomers were resolved from the parent compounds by LC using acidic eluents.[7,39]

In this paper we identify a group of epimerized AZA analogues found naturally in shellfish and phytoplankton, and report on their origin, stability, toxicity and relative response factors in LC-MS analysis. The potential consequences of AZA-epimerization for shellfish consumers are also briefly discussed.

MATERIALS AND METHODS

Chemicals. All solvents (pestican grade) were purchased from Labscan (Dublin, Ireland) and Caledon (Georgetown, ON, Canada). Distilled water was further purified using a Barnstead nanopure diamond UV purification system (Thermo Scientific, Iowa, USA). Sodium chloride (99+%), triethylamine (99%), ammonium acetate (97+%), ammonium formate (reagent grade), formic acid (>98%), and silica gel (10–40 μm, type H), were purchased from Sigma–Aldrich (Steinheim, Germany). Sodium chloride (99+%) and sodium periodate were purchased from Sigma Aldrich (St Louis, USA). Sephadex LH-20 was from GE Healthcare (Uppsala, Sweden), LiChroprep RP C8 (25–40 μm) was from Merck (Darmstadt, Germany), Luna phenyl-hexyl (15 μm) was from Phenomenex (Cheshire, UK), CD_3OH (99.5 atom-% D) was from Cambridge Isotope Laboratories (MA, USA), and CD_3OD and CD_3OH (100.0 and 99.8 atom-% D, respectively) were from Sigma–Aldrich (Steinheim, Germany). AZA CRMs were obtained from the National Research Council of Canada (Halifax, NS, Canada).

Culture toxin extraction. A sample (10 mL) of a culture of the Irish strain of *A. spinosum*[5] was transferred into a 15 mL centrifuge tube and centrifuged at 4,500 g for 5 min. The supernatant was decanted and the pellet was extracted with 1 mL of methanol by vortex mixing for 1 min followed by centrifugation for 5 min at 10,500 *g*. The extract was filtered through a glass Pasteur pipette plugged with cotton wool into an HPLC vial, for LC-MS analysis (method A).

Analysis of raw shellfish tissues. AZA-contaminated raw shellfish samples, tested as part of the routine monitoring programme in Ireland, were selected for analysis of epimers. The shellfish were shucked and homogenised using a Warring blender before extraction. Tissue samples (2 g) were extracted by vortex mixing for 1 min with 9 mL of methanol, centrifuged at (3,950 *g*) for 5 min, and the supernatant decanted into a 25 mL volumetric flask. The remaining pellet was further extracted using an Ultra Turrax homogenizer (IKA-Werke T25 at 11,000 rpm) for 1 min with an additional 9 mL of methanol, centrifuged at (3,950 *g*) for 5 min, and the supernatant decanted into the same 25 mL volumetric flask which was brought to volume with methanol. The extracts were analysed by LC-MS (method A).

Heat treatment of raw AZA-contaminated shellfish extracts and tissue. The extracts from above were transferred into centrifuge tubes and placed in a water bath (Grant Ltd, Cambridge, UK) at 90 °C for 10 min, removed, allowed to cool and transferred into HPLC vials for LC-MS analysis (method A). Aliquots (6 × 2 g) of whole tissue homogenate were weighed into centrifuge tubes, three of which were capped and placed in a water bath at 90 °C for 10 min, removed, allowed to cool and extracted (using the above extraction method) in parallel with the three unheated samples. The extracts were analyzed by LC-MS (method B).

Stability studies. Dilutions of fractions collected from the final step in the isolation of AZAs,[11] containing AZA1–3 and their epimers, were dissolved in acetonitrile–water (8:2) or in acetonitrile–water (8:2) to which 0.1% v/v formic acid or triethylamine had been added. Aliquots of the solutions were transferred to amber ampoules, flame-sealed under nitrogen, and stored at −18 °C, 20 °C and 40 °C for up to 7 days. The study was performed using a reverse isochronous strategy[40] and samples were analyzed under reproducibility conditions by LC-MS (method A) with specimens stored at −80 °C used as the control. An analogous study was performed in parallel using methanol (instead of acetonitrile–water) as solvent.

Isolation of 37-*epi*-AZA1 from shellfish. The isolation method employed is described in detail elsewhere.[11] Final separation of AZA1 from its epimer was achieved by semi-preparative HPLC (Shimadzu 10AVp) with photodiode array (PDA) detection at 210 nm using a Luna C8 column (5 μm, 250 × 10 mm) eluted with acetonitrile–water (11:9, plus 2 mM ammonium acetate) at 4 mL/min with a column temperature of 30 °C. AZA2, AZA3 and their 37-epimers were purified using the same system as for AZA1, but with a narrower-bore column (Cosmosil C18, 5 μm, 250 × 4.6 mm) eluted with acetonitrile–water (1:1, plus 2 mM ammonium acetate) at 1 mL/min. Purified AZAs were recovered by diluting the fractions with water (to 20% acetonitrile), loading on to solid-phase extraction (SPE) cartridges (Oasis HLB, 200 mg), washing with methanol–water (1:9, 10 mL) to remove the buffer, and eluting with methanol–water (9:1, 20 mL). However, the epimers were not sufficiently pure at this stage and there was some conversion (~ 8%) of the epimers back to the parent compound during the SPE step. Samples were therefore passed through semi preparative HPLC a second time, the acetonitrile was removed on a rotary evaporator at

20 °C, the AZAs extracted from the buffer with an equal volume of ethyl acetate, and the solvent was removed on a rotary evaporator at 20 °C to give the epimers as colorless solids.

Periodate cleavage. Dilutions of fractions collected from the final step in the isolation procedure, containing both parent analogue and its epimer, were dissolved in methanol. To 100 μL of sample was added 50 μL of 0.2 M sodium periodate solution, and the reaction analyzed immediately by LC-MS (method A) and again at intervals over a 2 h period, but including traces at *m/z* 448.4 (for the AZA1 and AZA2 oxidation product) and at *m*/*z* 434.4 (for the AZA3 oxidation product). As a control, the sodium periodate solution was replaced by water.

Incorporation of deuterium from CH_3OD. An aliquot (0.5 mL) from the final step in the isolation procedure, containing both AZA1 and 37-*epi*-AZA1, was evaporated under nitrogen, taken up in 0.5 mL CH_3OD, stored at 40 °C, and aliquots analyzed periodically over 10 days by LC-MS (method A) for *m/z* 842.5, *m/z* 843.5 and *m/z* 844.5 to monitor deuterium incorporation. An aliquot (0.2 mL) of the partially deuterated sample was evaporated under nitrogen, dissolved in methanol (40 μL) and added to 1 M phosphate buffered saline (PBS) (160 μL). The sample was stored at 40 °C and analyzed periodically over 4 days by LC-MS (method A) for *m/z* 842.5, *m/z* 843.5 and *m/z* 844.5 to monitor loss of deuterium.

LC-MS analysis.

Method A. A Micromass Ultima time-of-flight (QToF) mass spectrometer equipped with a z-spray ESI source and coupled to a Waters 2795 LC was used for this method. Separation was performed on a 5 μm, 150 × 2 mm Luna C18 (2) column (Phenomenex, UK) operated at 30 °C, injecting 5 μL samples. A binary mobile phase of water (A) and acetonitrile–water (95:5) (B), each containing 5 mM ammonium acetate (pH 6.8), was used isocratically (A:B, 35:65) at a flow rate of 0.35 mL/min. The QToF was operated in product ion scan mode, where the precursor ions selected were: *m/z* 842.5 (AZA1 and AZA6); 856.5 (AZA2); and 828.5 (AZA3), in positive ionization mode. The cone voltage was 40 V and the collision voltage was 50 V, the cone and desolvation gas flows were set at 100 and 750 L/h, respectively, and the source temperature was 150 °C.

Method B. An Agilent 1200 LC system (Agilent Inc., Palo Alta, CA, USA) connected to an API4000 QTRAP mass spectrometer (AB Sciex, Concord, ON, Canada) equipped with a Turbospray ionization source was used for this method. Separation was performed on a 2.5 μm, 2.1 × 50 mm, Luna C18(2) HST column (Phenomenex, Torrance, CA, USA)

operated at 15 °C, injecting 1–5 µL samples. A binary mobile phase of water (A) and acetonitrile–water (95:5) (B), each containing 5 mM ammonium acetate (pH 6.8), was used, with a gradient from 25 to 100% B over 5 min at 0.35 mL/min and held at 100% B for 2 min before re-equilibration for the next run. The MS was operated in positive ion selected reaction monitoring (SRM) mode for the following transitions: *m/z* 842.5→672.5 (AZA1); *m/z* 856.5→672.5 (AZA2); *m/z* 828.5→658.5 (AZA3) and *m/z* 842.5→658.5 (AZA6) with collision energy 70 eV. Typical parameters were electrospray voltage 5500 V, source temperature 400 °C, and declustering potential 70 eV.

Method C. For the relative molar response study on AZA1 and 37-*epi*-AZA1, samples were analysed using a number of LC-MS/MS methods. Analyses were performed on an Agilent 1200 LC system (Agilent Inc., Palo Alta, CA, USA) connected to an API4000 QTRAP mass spectrometer (AB Sciex, Concord, ON, Canada) equipped with a Turbospray ionization source. The MS was operated in positive ion mode and SRM for the following transitions: *m/z* 842.5→824.5/806.5/672.4/654.4/462.3/362.3 (AZA1 and 37-*epi*-AZA1), with collision energies of 45 to 70 eV. For selected ion monitoring (SIM) experiments, *m/z* 842.5 ($[M+H]^+$) was analyzed.

Method C(i) Gradient elution with a neutral mobile phase was run as described for method B.

Method C(ii) Isocratic elution with a neutral mobile phase was run on the same Luna column using 60% B at 0.3 mL/min.

Method C(iii) Gradient elution with acidic mobile phase was run on the same Luna column but eluting with water (A) and acetonitrile–water (95:5) (B), each containing 50 mM formic acid and 2 mM ammonium formate. Linear gradient elution was run from 25 to 100% B over 5 min at 0.3 mL/min and held at 100% B for 2 min, before re-equilibration for the next run.

Method C(iv) Isocratic elution with the acidic mobile phase was run on the same Luna column using 55% B at 0.3 mL/min.

High resolution MS/MS spectra. Aliquots (~ 5 µL) of AZA1 and -2 after NMR analysis in CD_3OH and CD_3OD, respectively, were diluted with 500 µL MeOH to remove rapidly exchangeable OD- and ND-groups, evaporated to dryness under N_2, and dissolved in 1 mL acetonitrile for analysis. High resolution MS/MS spectra of the $[MH+1]^+$ ions (*m/z* 843.5 and 857.5, respectively) of AZA1 and -2 (Supporting Information) during infusion of the solutions into a Q Exactive mass spectrometer (Thermo Scientific) using ESI in positive ion mode with mass-selection width set to *m/z* 0.4 and scan range *m/z* 150–900. The normalized

collision energy was 30 eV, resolution was set to 140 K, with capillary temperature 320 °C, S-lens RF level 50, spray voltage 3.8 kV, and sheath gas and auxiliary gas at 45 and 10 units respectively.

NMR Spectroscopy

Structural Elucidation. Structural determinations were performed by analysis of ^{1}H, COSY, TOCSY, SELTOCSY, NOESY, ROESY, SELROESY, ^{13}C, DEPT135, HSQC and HMBC spectra using Bruker Avance I or Avance II 600 MHz spectrometers equipped with a TCI cryoprobe and Z-gradient coils. Samples of AZA1 (1 mg), 37-*epi*-AZA1 (0.1 mg) and AZA2 (1 mg) were dissolved in ~ 0.5 mL CD_3OD or CD_3OH at 30 °C, and chemical shifts were referenced to internal CHD_2OD or CHD_2OH (both 3.31 ppm), or CD_3OD or CD_3OH (49.0 ppm). Single- or double-frequency pre-saturation of solvent resonances was performed using continuous wave and/or excitation sculpting as required.

Quantitative NMR (qNMR). Quantitation of AZA1 and 37-*epi*-AZA1 by NMR was performed on a Bruker Avance II 600 spectrometer using a BBI probe (5 mm) and operating at room temperature. Purified samples dissolved in CD_3OH were measured against external standards of caffeine dissolved in H_2O (4.10 mM) as described previously for AZA CRMs[32] using techniques described previously by Burton et al.[41]

Toxicology

Cell Culturing. Non-adherent human Jurkat E6-1 T lymphocyte cells (American Type Culture Collection TIB-152; Manassas, VA, USA) were grown as described by Twiner et al.[22,26] Briefly, cells were grown in RPMI medium (cat. #11875-093, Invitrogen, CA, USA) supplemented with 10% (v/v) fetal bovine serum (FBS; cat. #26140, Invitrogen, CA, USA) and maintained in a humidified incubator (Sanyo 18AIC-UV) with 5% CO_2 in air at 37 °C. Cells were subcultured with fresh medium at an inoculum ratio of 1:4 every 3 to 4 days by transferring 2.5 mL of cells to 7.5 mL of fresh supplemented medium in 75 cm^3 screw cap culture flasks.

Cytotoxicity assay. The effect of AZA1 and 37-*epi*-AZA1 on viability of Jurkat T lymphocyte cells was determined. Jurkat T lymphocytes were selected based on initial *in vivo* observations[15], cell sensitivity following extensive *in vitro* cytotoxicity screening experiments[22], and for comparative purposes to other AZA analogues for which potencies have been determined using this assay.[26,29] The Jurkat T lymphocyte cell line was grown as described above and cells were seeded in 100 μL of the supplemented medium at 35,000 cells

per well in black, sterile, 96-well culture plates for 24 h to allow for recovery and settling. The AZA analogues were added at various concentrations for 24, 48, and 72 h of continuous exposure prior to assessment of cytotoxicity. The final concentrations of AZA1 ranged from 9.5×10^{-8} to 5×10^{-12} M, and the final concentrations of 37-*epi*-AZA1 ranged from 7.6×10^{-7} to 5×10^{-12} M. Parallel controls of equivalent amounts of methanol/PBS were used to normalize the viability data for each treatment. Following exposure of the cells to the AZA analogues for the specified period of time, cellular viability/cytotoxicity was assessed using the MTS (3-(4,5-dimethylthiazol-2-yl)-5-(3-carboxymethoxyphenyl)-2-(4-sulfophenyl)-2H-tetrazolium) assay (Promega Biosciences, San Luis Obispo, CA, USA; cat. no. G5421). Each well received 10 μL of the MTS solution, the cells were incubated for 4 h at 37 °C, and absorbance at 485 nm was measured (FluoStar microplate reader, BMG Lab Technologies). Data are presented as means ± standard error of three separate experiments (n = 3). In addition, each cytotoxicity experiment was performed using duplicate wells. Cytotoxicity data were blank-corrected and normalized to the control (% viability) and plotted using GraphPad Prism (ver. 5.0c, San Diego, USA).

*Collection of Samples for Metabolites***.** Samples were taken throughout the course of the toxicology experiments to determine AZA analogue stability and/or metabolite composition. In parallel with the cytotoxicity experiments outlined above, these experiments were conducted using AZA1 and 37-*epi*-AZA1 with initial concentrations in each well of 94.8 and 767 nM, respectively. Samples were taken directly from the 96-well plates containing T lymphocyte cells at 0, 24, 48, and 72 h following the addition of the AZAs. The experiments were conducted in triplicate and also repeated in the absence of cells. At the given time, the entire volume (100 μL) of the well contents were transferred to a glass vial and then immediately frozen at −70 °C. Direct analysis of the samples was performed by LC-MS (method B).

RESULTS AND DISCUSSION

Observation and formation. The AZA isomers were first observed during the development of analytical methods for the measurement of a mussel tissue matrix CRM for AZAs. When LC conditions were switched from using an acidic mobile phase to a neutral one, additional isomeric peaks were resolved (Figure 2). Analysis of a fresh *A. spinosum* culture showed no detectable AZA1 and AZA2 isomers, while extracts of raw shellfish (*M. edulis* and *C. gigas*) contaminated with AZAs (0.08–4.8 μg/g) showed the presence of only minor amounts (< 2%). However, when the extracts were heated to 90 °C for 10 min, the concentration of isomers increased to 6–15% of the parent compounds (Figure 3).

These results strongly suggested that the isomers are heat-promoted conversion products and further highlights the fact that the chemical profile of these toxins in shellfish can change significantly during cooking. Previous studies have shown that levels of certain AZAs (e.g., AZA3) increased dramatically upon cooking as a result of other AZA analogues undergoing decarboxylation.[6]

Stability. Short-term stability studies were performed for the isomers of AZA1–3 using dilutions of fractions collected from the isolation step for AZAs,[11] at −18 °C, ~ 20 °C and 40 °C in two solvents and under weakly acidic and basic conditions over a 7 day period. The results showed that the isomers were stable at freezer and room temperatures, while at higher temperatures (40 °C) they converted back to the parent analogues (Figure 4). Greatest stability is observed under weakly basic conditions while the weakly acidic conditions increased instability. The isomers were significantly more stable in aqueous acetonitrile than in methanol, with the rate of conversion being twice as fast in methanol (Figure 4). Isomerization of AZA2 was observed during NMR analysis in CD_3OD, but appeared to cease upon addition of 0.1% v/v d_5-pyridine.

The stability data indicated that equilibrium is reached at ~ 16% isomer (Table 1). Conversion of the isomer to the parent analogue was faster for AZA3 relative to AZA1 and AZA2 (Table 1). In the presence of methanol, methyl ketals[11] were also formed at the higher temperatures, particularly so for AZA3 and under the acidic conditions (Supporting Information).

The stability studies provided valuable information with respect to handling of the samples. The fact that the isomers were relatively stable at room temperature over a number of days meant that there was no conversion whilst performing the semi preparative HPLC step. Procedures that are normally performed at higher temperatures (evaporation of solvents and NMR spectroscopy) could be performed at lower temperatures to deal with this instability. Thus, evaporation steps were carried out at ≤ 20 °C and qNMR was performed at 20 °C.

Previous studies on AZAs showed that the stability of AZA1 and AZA6 was significantly improved when stored in acetonitrile–water (8:2) when compared to methanol.[11] Experiments performed in this study confirm these findings. Not only was there faster conversion of isomers to the parent analogues in methanol, but the formation of methyl ketals[11] was observed in methanol and was promoted under the acidic conditions.

Purification. AZAs were isolated from mussels to obtain sufficient quantities for the preparation of reference materials and for toxicological studies.[11] During the semi-preparative HPLC purification (7th step) of the isolation procedure, peaks eluting close to the main AZA1–3 peaks were collected separately, and through LC-MS analysis shown to be mixtures of the parent analogue and its isomer. A purified sample of the AZA1 isomer was obtained by performing an additional HPLC separation step. Analysis of the isomer fraction collected immediately after the semi preparative step showed that < 1% of the parent analogue was present. However, after the sample was passed through the SPE cartridge to remove the buffer, significant conversion to the parent compound had occurred (~ 8%). The use of other SPE stationary phases (C18 and C8) also had the same effect. Evaporation of the organic solvent from the sample at ≤ 20 °C and subsequent extraction of the sample with ethyl acetate proved to be effective at maintaining the stability of the isomer with no conversion being observed. Sufficient AZA1 isomer (~ 150 µg) with adequate purity (containing ≤ 1.5% AZA1) was isolated for analysis by NMR (both structural and quantitative). Small amounts of the AZA2 and AZA3 isomers were also isolated but not in sufficient quantities for NMR analyses. Nevertheless, sufficient levels of isomers were present in stored NMR samples of AZAs 1–3 to permit partial NMR signal assignments.

Previous AZA purification procedures employed an acidic mobile phase in the final purification step.[29,32] Therefore, any isomer present would have been collected as part of the

parent analogue peak. The procedure used in the present study employed a neutral mobile phase, which enabled the isomers to be resolved from the parent analogue peaks and permitted their purification. In addition to the AZA1–3 isomers, a fraction containing the equivalent isomer of AZA6 was also collected which suggests these isomers exist for all the known AZA analogues.

Structure determination

LC-MS. The only clear differences in the LC-MS spectra between the parent analogue and its isomer were changes to the ratio of the water loss, retro Diels–Alder (RDA) (*m*/*z* 672/654) and the relative intensity of the *m*/*z* 462 fragment ions (Figure 5).

Periodate cleavage. Periodate cleaves the diol moiety of AZAs at C-20/21 to produce a lactone.[6,7,11] In methanol, AZA1 and its isomer were both cleaved by periodate at essentially the same rate (Supporting Information), giving products with the same mass but having different retention times. This shows that the isomer cannot simply be the 21-*epi*-AZA1, because C-21 is oxidized to a carbonyl group during cleavage and could not therefore give rise to isomeric oxidation products. Rather, the isomer of AZA1 must result from structural modification in C-22–C-40.

NMR spectroscopy. The structure determination of AZAs and their isomers is complicated by the known, but hitherto poorly defined, pH dependency of the majority of the proton and carbon atoms of the penultimate six membered nitrogen-containing ring and the five membered furanosyl ring attached to it.[11] For example, Ofuji et al.[9] have reported shifts of 2.83 ppm and 2.91 ppm for the H-40 methylene resonances of AZA2 in CD_3OD, whereas we observed chemical shifts ranging between 2.54 and 2.80 ppm for these protons in the NMR spectra of two specimens of AZA2 (Table 2) and in the spectra of other AZAs examined in our laboratory. The NMR spectral data originally reported for AZA1–5[3,9,10] were obtained from CD_3OD containing 0.5% v/v CD_3CO_2D in order to sharpen some of the resonances in the region around the amino group (M. Satake, University of Tokyo, Japan, personal communication). However, given that we found the isomerization of AZAs in methanol to be catalyzed by dilute acetic acid, structural NMR analysis of the AZA-isomers in this CD_3OD containing CD_3CO_2D was not considered appropriate. We therefore used CD_3OD without added acid, although as a consequence of this some of the chemical shifts varied significantly from sample-to-sample, presumably because the degree of protonation of the amino group varied slightly from isolation-to-isolation.

A further complication in the structural analysis of AZAs is that the chemical shift of H-20 is also sensitive to the extent to which the terminal ring nitrogen atom is protonated. We have observed shifts for this proton in the range 3.55 to 3.86 ppm in specimens of AZA1 and AZA2, and some other AZAs examined in our laboratory whereas Ofuji et al.[9,10] have reported shifts in the vicinity of 3.94 ppm for the mildly acidified solutions of AZAs that they examined. Notwithstanding the varying H-20 chemical shifts, an identical series of ROESY correlations, indicative of a common C-20 stereochemistry, was observed between H-20 and the nearby H-18a, H-19, H-22 and 22-CH_3 protons.

The sensitivity of H-20 chemical shifts to the varying extent of *N*-protonation can be interpreted as indicating the preferred solution conformation of AZAs as one in which the proton (or protons) attached to the terminal ring *N*-atom are positioned towards the central C-20 atom. Detailed analyses of 1D-SELROESY and 2D-ROESY data verified this proposal. In particular, irrespective of the chemical shift of the H-20 signal and of protons attached to carbon atoms in the C-31−C-40 portion of AZAs (which vary from specimen to specimen), moderate to strong inter-ring ROESY correlations were observed from H-40_{eq} to H-19, and to the pro-*Z* 26=CH_2 proton, together with ROESY correlations arising from suitably oriented terminal-ring protons. These correlations are consistent with a preferred solution of AZAs amino group and H-40 protons orientated towards H-19. The known pH sensitivity of some of the protons in close proximity to the terminal ring *N*-atom, and remote from it (H-20), can now be rationalized, since variations in the degree of protonation of the nitrogen atom will also influence the chemical shift of the H-20 proton. The resulting steric hindrance of the amino group in this conformation may also explain its observed lack of reactivity towards alkylation and acylation.[42]

Because LC-MS studies had shown that AZAs underwent slow isomerization in methanol, preliminary NMR investigations of the isomers were able to be performed on samples in deuteromethanol containing both the parent analogue and its isomer (Table 3). This has the advantage that chemical shifts for both the parent AZA and its isomer can be directly compared, despite the sensitivity of some of the chemical shifts towards pH. However, signals from the parent compound were often greater than 20-fold more intense than those of the isomer, and many of these signals overlapped signals from the isomer, making structural analysis challenging and only partial assignment of isomer resonances was possible via analysis of 1D and 2D NMR spectra. The stability data obtained during this work eventually allowed isolation of the isomer of AZA1 in sufficient amounts (~ 150 μg) and purity (> 95%) for structure elucidation by NMR spectroscopy.

The chemical shifts established for the ring-A–D carbons and protons for the AZA1 and AZA2 isomers were essentially identical to those which we determined for AZA1 or AZA2, respectively, in CD_3OD, CD_3OH or d_6-DMSO, and in accordance with those reported by Ofuji et al.[9] However, the assignments for resonances from the 7- and 9- positions were reversed[11] due to the revision of the position of the ring-A double bond from the 8(9)-position to the 7(8)-position as established by synthesis.[43–45] In addition, the original assignments for the 11- and 12-positions[9] were reversed based on HMBC correlations observed for the methylene protons of AZA2 that resonate at 2.33 and 2.16 ppm. HSQC data showed that those protons were attached to the methylene carbons resonating at 33.2 and 37.4 ppm, respectively. In the HMBC spectrum of AZA2, the proton signal at 2.33 ppm exhibited an HMBC correlation to the C-14 methine carbon signal, which resonated at 31.0 ppm, while the proton signal at 2.16 ppm exhibited an HMBC correlation to the C-9 methylene carbon at 40.4 ppm (mistakenly assigned as the C-7 resonance by Ofuji et al[9] due to the incorrect position of the ring-A double bond). These correlations are consistent with methylene proton signals at 2.33 ppm and 2.16 ppm showing ^3J correlations to C-14 (31.0 ppm) and C-9 (40.3 ppm), respectively, rather than ^4J correlations (rarely seen in HMBC spectra). Thus, these HMBC correlations indicated that the proton signal at 2.33 ppm is from H-12, and that the signal at 2.16 ppm is from H-11, and consequently that their carbon signals at 33.2 and 37.4 ppm arise from C-12 and C-11, respectively. The equivalent HMBC correlations were also observed for AZA1 and its isomer, indicating that this re-assignment applies to other AZAs.

Other than for the reversal of the Ofuji et al.'s assignments for the 11- and 12-methylene groups, proton and carbon chemical shifts, ^{1}H coupling constants observed in ^{1}H NMR or SELTOCSY experiments, together with TOCSY and ROESY correlations observed for the isomers of AZA1 and AZA2 (where resolved from those of AZA2), were consistent with ring-A–D portions the structures of the isomers being the same as that reported for AZA1 and AZA2, respectively.

Knowledge of both the pH dependency of some of the chemical shifts and the preferred solution confirmation of AZAs, as revealed by inter ring ROESY correlations, facilitated the structure determination of the AZA1 isomer. In particular, the AZA1 isomer exhibited a series of ROESY correlations (e.g. H-20 (3.50 ppm) to H-19 (4.45 ppm), H-16 (3.91 ppm), H-22 (2.30 ppm), H-18a (2.07 ppm), and 22-Me (0.82 ppm); and H-40$_{eq}$ (2.62 ppm) to the pro-*Z* 26=CH_2 proton (5.28 ppm), H-19 (4.43 ppm) and 39-Me (0.88 ppm)) similar to those observed for AZA1 and AZA2. However there were ROESY correlations shown by other

terminal ring protons, most notably between the 37-Me (1.06 ppm) and H-39 (1.84 ppm), H-38a (1.44 ppm) and H-35a/b (2.11 ppm)) which were consistent with axial orientation of the 37-Me group in the AZA1 isomer rather than the equatorial orientation in AZA1 and all other known AZAs (Figure 1).

This deduction was supported by the occurrence of the C-39 methine carbon signal of the AZA1 isomer at 25.0 ppm compared to 29.8 ppm in AZA1 (Table 3). The upfield shift observed for C39 is reminiscent of that exhibited by C-37 of DTX2 (21.0 ppm), which possesses an axial 35-methyl group relative to that of C-37 in DTX1 (27.5 ppm) which possesses an equatorial 35-methyl group.[46]

Confirmation of 37-epimerization (Figure 6), and the identification of the axial and equatorial H-38 and H-40 methylene protons of the epimer of AZA1 (and AZA2), was obtained via analyses of the coupling constants exhibited by the H-38 and H-40 methylene protons, revealed in contour plots and slices extracted from 2D-HSQC and TOSCY spectra, the resolution of which for protons in 6-membered rings was sufficient to resolve large $^{2}J_{gem}$ and $^{3}J_{ax–ax}$ couplings (~ 10–12 Hz) but not the smaller $^{3}J_{ax–eq}$ or $^{3}J_{eq–eq}$ couplings (typically 3–4 Hz or less). In a 1D-SELTOCSY spectrum of partially epimerized AZA1 obtained at the resonance frequency of the 37-Me of 37-*epi*-AZA1 (1.06 ppm) (Figure 1), H-38_{ax} appeared as a well-defined triplet of doublets due to $^{2}J_{H\text{-}38ax–H\text{-}38eq}$ and $^{3}J_{H\text{-}38ax–H\text{-}39ax}$ couplings of 10–12 Hz. In contrast, H-38_{ax} appeared as a quartet-like signal in the 2D-HSQC, TOCSY and 1D-SELTOCSY spectra of AZA1 and AZA2 due to $^{2}J_{H\text{-}38ax–H\text{-}38eq}$, $^{3}J_{H\text{-}38ax–H\text{-}39ax}$ and $^{3}J_{H\text{-}38ax–H\text{-}37ax}$ couplings of ~ 10–12 Hz. The H-38_{eq} signal of each the compounds appeared as a doublet since only the large $^{2}J_{H\text{-}38ax–H\text{-}38eq}$ coupling of ~ 10–12 Hz and not smaller $^{3}J_{ax–eq}$ or $^{3}J_{eq–eq}$ couplings were resolved in HSQC or TOCSY slices (Figure 1). Similar observations were made for partially epimerized specimens of AZA2 (Table 2) as well as for all other AZAs studied (unpublished observations).

The axially and equatorially oriented H-40 protons of AZAs were identified similarly, since in the 2D-HSQC and TOCSY spectra H-40_{ax} appeared as a triplet-like signal due to well resolved $^{2}J_{H\text{-}40ax–H\text{-}40eq}$ and $^{3}J_{H\text{-}40ax–H\text{-}39ax}$ couplings while the H-40_{eq} appeared as a doublet signal due to resolution in HSQC spectra of only the larger $^{2}J_{H\text{-}40ax–H\text{-}40eq}$ coupling and not the smaller $^{3}J_{H\text{-}40eq–H\text{-}39ax}$ coupling (Figure 1). These observations were supported by NoE correlations observed in the ROESY and SELROESY spectra of AZA1, 37-*epi*-AZA1 (Figure 7), and in a mixed sample of AZA2 and its epimer (data not shown).

It was apparent from the inter-ring ROESY correlations that the H-40$_{eq}$ protons in AZA1 and 37-*epi*-AZA1 exhibited to H-19 to the pro-*Z* 26=CH_2, that the C-36 configuration of 37-*epi*-AZA1 was as in AZA1 since the foregoing pair of ROESY correlations would not have been observed for 37-*epi*-AZA1 had it also been epimerized at C-36.

The analyses of stereochemically definitive H-38 and H-40 coupling constants was enhanced by the acquisition of NMR spectral data for AZA1 and 37-*epi*-AZA1 in CD_3OH, including 1H, 2D-COSY, TOCSY, ROESY and HSQC data, with pre-saturation of the protonated CD_3OH/HOD signals. This appreciably sharpened the H-40 methylene protons of the respective compounds by preventing the NH proton (or the protonated variant of it) from exchanging deuterium with the solvent and the consequent line broadening effect due to $^3J_{D–C–C–H}$ coupling(s) between the N–D (or N–D_2^+) and H-40 methylene protons. Essentially identical ^{1}H (to within 0.01 ppm) and ^{13}C shifts (to within 0.1 ppm) were obtained in CD_3OD and CD_3OH. On the other hand, a significant difference (and in some cases beneficial resolution of overlapped methylene proton signals) was observed when d_6-DMSO was substituted for CD_3OD or CD_3OH (Table 3).

Epimerization at C-37 presumably proceeds as shown in Scheme 1. Consistent with this was the observation that deuterium was rapidly incorporated at C-37 of the epimer formed during isomerisation of AZA1 and AZA2 in CD_3OD, together with a slower incorporation of deuterium at the pro-*S* position at C-35 (2.34 ppm in AZA2). Examination of AZA2 after NMR in CD_3OD using high resolution MS/MS of the *m*/*z* 857.5 ion confirmed the presence of deuterium (as well as ^{13}C) in the C-33–C-40 fragment.

To verify this finding, a sample containing 37-*epi*-AZA1 and AZA1 was stored in CH_3OD at 40 °C and analyzed periodically by LC-MS. The incorporation of deuterium was observed via the appearance of fragment peaks with extra mass (Supporting Information). Intensity changes observed in HSQC spectra (Supporting information) indicated rapid uptake a first deuterium and a somewhat slower incorporation of a second at H-37 and H-35$_S$, respectively, with a very slow (possibly due to steric effects) incorporation of a third deuterium at H-35$_R$.

After 10 days of storage in CH_3OD, the deuterated sample was evaporated, taken up in PBS (with 20% methanol), and stored at 40 °C to assess the rate of deuterium loss from the structure in this medium (Supporting Information). Deuterium was washed out fairly rapidly, with ~ 60% of the original deuterium remaining after 4 days (Supporting Information). In addition, it was observed that the AZA epimer converted back to AZA1 at a much faster rate in the PBS solution after 24 h (80% conversion) than in methanol (14% conversion). These

findings are significant as they could enable the production of stable isotope-labelled internal standards that could be used to compensate for matrix effects and increase the accuracy of LC-MS quantitation. Furthermore, it might be possible to produce tritium-labelled AZAs for biochemical investigations.

Relative Molar Response Study. 37-*epi*-AZA1 that had been isolated and purified for structural elucidation was quantitated by qNMR. The molar response of the epimer was assessed against purified AZA1[11] that had also been quantitated by qNMR. Accurate working standards were then prepared by diluting the qNMR stock solutions in high purity degassed methanol. The concentrations of the working solutions were 1.3 µM for AZA1, and 1.2 µM for 37-*epi*-AZA1. The anthryldiazomethane (ADAM) derivatization method for LC-FLD of AZAs[42] was applied to the AZA1 and 37-*epi*-AZA1 standards to provide supporting information for the qNMR data. However, due to instability of 37-*epi*-AZA1, a significant proportion of it converted back to AZA1 under the derivatization conditions and the ADAM results for the epimer would therefore not be reliable quantitatively (Supporting Information).

A number of mass spectrometric experiments were carried out (LC-MS method C) in order to determine the molar response of 37-*epi*-AZA1 relative to AZA1. The results are summarized in Table 4. Although the proportion of epimer present in samples is approximately 2–16%, and may be considered relatively low, it is still important to understand any potential differences in response in the MS detection of the epimers when compared to the parent AZA analogues. When establishing the relative molar responses of different compounds in LC-MS the mobile phase composition can influence the ionization efficiency, therefore it is important to test under isocratic conditions if possible. Differences can also arise due to the MS detection mode. While SIM detection depends only on the ionization efficiency of the compounds in the ESI source, and the transport of the ions through to the quadrupole, detection in SRM can also be affected by differences in the fragmentation of compounds. Therefore, to establish baseline response factors initial analyses were done using isocratic elution with detection in SIM mode. SRM is more commonly used in routine/regulatory LC-MS/MS analysis of lipophilic toxins, therefore the standards were also analysed in SRM mode. In most cases the response factor of the 37-*epi*-AZA1 was not considerably different from that of AZA1. The isocratic elution SIM data obtained for AZA1 and 37-*epi*-AZA1 was consistent between acidic and neutral pH mobile phases and the results suggest that 37-*epi*-AZA1 has a slightly lower response than AZA1 when analysed under these conditions (0.94 relative to AZA1). In all SRM transitions *m/z* 842.5 was selected in Q1, and following fragmentation a variety of ions were selected in Q3. The data shows that the SRM transition

selected for analysis of 37-*epi*-AZA1 could have a significant impact on quantitation when using an AZA1 standard (Table 4). Although the initial collision induced water losses (*m/z* 824 and 806) are not ideal transitions for confirmatory purposes, due to the higher probability of interferences from isobaric species, they both show response factors for 37-*epi*-AZA1 within 10% of those observed when using the same transitions for AZA1. The *m/z* 672 fragment that results from RDA cleavage of the A-ring also gave a similar response factor. However, the subsequent water loss from this RDA fragment (*m/z* 654) gave a much lower response for 37-*epi*-AZA1 relative to AZA1 (~ 0.57). This difference correlates to one of the major differences observed in the product ion spectrum of both compounds (Figure 5). The intensity of the *m/z* 654 ion is much reduced in the product ion spectrum of 37-*epi*-AZA1, which is probably due to this water loss occurring near C-21, Figure 5. Therefore, the 842→654 transition is not ideal for quantitation of AZA1 and 37-*epi*-AZA1 under conditions where they are not resolved. A lower response factor was also observed when using *m/z* 462 as the Q3 ion in SRM (0.76 relative to AZA1), which correlates with the reduced intensity of this ion in the product ion spectrum of 37-*epi*-AZA1 (Figure 5). The *m/z* 362 ion is frequently used as a confirmatory transition in SRM analysis of regulated AZAs and a slightly higher response factor was observed when using this as the Q3 ion in SRM analysis of 37-*epi*-AZA1. With an acidic mobile phase (pH 2.3) the use of gradient or isocratic elution had no impact on the relative response of 37-*epi*-AZA1. This is because AZA1 and 37-*epi*-AZA1 co-elute at this pH, and are being ionized in the ESI source at the same mobile phase strength. However, it can be seen that on average the relative molar response of 37-*epi*-AZA1 relative to AZA1 was slightly higher when using neutral mobile phase compared to acidic. This is because 37-*epi*-AZA1 is resolved from AZA1 at the neutral pH, eluting later. The increased organic content of the mobile phase when 37-*epi*-AZA1 elutes conceivably causes the slightly higher response observed.

Toxicology. Of all the functional assays developed for AZAs, the Jurkat T lymphocyte cell assay was found to be the most sensitive,[29] and was therefore chosen to assess the toxicity of 37-*epi*-AZA1. In this assay, cells initially respond to AZAs by a reduction in membrane integrity, organelle protrusion concurrent with flattening of cells, the retraction of their pseudopodia or lamellipodia, followed by protracted cell lysis.[22]

In a manner not unlike many other AZA analogues 37-*epi*-AZA1 was cytotoxic to Jurkat T lymphocyte cells in a time- and concentration-dependent manner (Figure 8). The 37-*epi*-AZA1 was shown to be 5.1-fold more potent than the parent AZA1 (Table 5) making it comparable in potency (*in vitro*) to AZA2 and AZA3 (8.3- and 4.5-fold more potent than

AZA1, respectively).[26] However, this work has shown the epimer to be highly unstable, rapidly converting back to its parent analogue at temperatures > 20 °C, and since all of the cytotoxicity experiments were run for a protracted period of time (up to 72 h) at 37 °C, it was anticipated that there could be significant conversion of the epimer back to AZA1. As such, samples were taken frequently throughout the course of the study and subsequently analysed by LC-MS to assess for these (or other) structural changes.

The analysis showed that the samples taken immediately after injection (i.e., t = 0 h) consisted of 94% 37-*epi*-AZA1 and 6% AZA1. After 24 h, considerable conversion of the epimer to AZA1 had taken place (73% AZA1), with nearly full equilibration between 48 and 72 h (~ 12% isomer). Similar conversion rates were observed in the stability study in which the deuterated AZA epimer mix was stored in a methanol:PBS solution at 40 °C. In parallel, analysis of the AZA1 sample at t = 0 showed that 3% of the isomer was present while after 24 h the amount increased to 11% with apparent equilibration being achieved after 48 h at 12% (Table 5). Assuming the total AZAs remain constant over the course of the experiment, we have shown that there was little to no metabolism or irreversible binding (e.g., to protein or plastic) of the AZAs (Table 6).

The conversion of 37-*epi*-AZA1 to the parent compound at 24 h (~ 75% AZA1) was surprising given the significantly higher potency determined for the epimer. However, previous experiments using this assay[13] and other *in vitro* methods by various investigators[25,47,48] indicate that the toxic effects of AZAs are immediately elicited and irreversible, which could explain the increased potency of the 37-*epi*-AZA1 despite its instability under the conditions tested. Although these laboratory findings suggest that the epimeric forms of AZA may present more of a toxicological hazard than the parent molecules and may be important from a monitoring perspective, we do not yet know the stability and/or contribution of these analogues *in situ*, nor whether a similar structure–activity relationship applies *in vivo*.

CONCLUSION

37-Epimers of AZA1–3 and AZA6 were detected in tissue CRMs using a neutral mobile phase with LC-MS detection. The proportion of the epimers ranged from 2–16%, with proportions increasing following the application of heat. Stability studies showed that the epimers convert at higher temperatures back to the parent analogue and that equilibrium in

solution is reached at ~ 16%. Sufficient amounts of 37-*epi*-AZA1 were isolated to enable full structural elucidation by NMR showing it to differ from AZA1 in the orientation of the methyl group at the C-37 position. Although only 37-*epi*-AZA1 was fully characterized it is highly likely that the epimers of AZA2, AZA3 and AZA6 have the same stereochemistry. Work currently being undertaken suggests that these epimers exist for all AZAs. Relative molar response factor studies by LC-MS revealed no major difference in response factors between the two compounds when analysed by SIM or SRM when the typical transitions are used (842→824, 842→672 and 842→362), but a significant difference was observed for the 842→654 transition and this is therefore not recommended for quantitative analysis of AZAs. 37-*epi*-AZA1 was 5.1 times more cytotoxic to Jurkat T lymphocyte cells than AZA1. Consequently, full equilibration (to 16% 37-*epi*-AZA1) of a sample containing AZA1 could be expected to increase the sample's toxicity in this assay by ~ 1.7-fold, assuming that the epimer has the same toxicological mechanism of action as AZA1. Furthermore, the observation that the rate of epimerization is increased in weakly acidic solutions may be of relevance to toxicity via oral exposure. This and previous[6] studies thus highlight the importance of assessing toxin profiles in cooked shellfish (typically shellfish are cooked before consumption) due to toxin conversions, as well as the need for further toxicological studies (*in vitro* and *in vivo*) to be performed on the conversion products such as these AZA-epimers.

ASSOCIATED CONTENT

AUTHOR INFORMATION

Corresponding author

*Tel: (+353) 91 387376. Fax: (+353) 91 387201. Email: jane.kilcoyne@marine.ie

Funding

This project (PBA/AF/08/001(01) was carried out under the *Sea Change* strategy with the support of the Marine Institute and the Marine Research Sub-Programme of the National Development Plan 2007-2013, co-financed under the European Regional Development Fund and supported in part by a Marie Curie International Incoming Fellowship within the seventh European Community Framework Programme (FP7/2007-2013) under grant agreement no. 221117. Funds were also provided by the University of Michigan-Dearborn's Office of Research and Sponsored Programs.

Notes

The authors declare no competing financial interest.

ACKNOWLEDGEMENTS

We thank the biotoxin chemistry team as well as Rafael Salas and Shane Shannon from the phytoplankton team (supply of the *A. spinosum*) at the Marine Institute (Galway, Ireland) and the staff of Biotoxin Metrology at NRC (Halifax, Nova Scotia, Canada), in particular Sabrina Giddings for her assistance in the laboratory.

Supporting information available

LC-MS chromatogram showing effect of pH on separation of 37-*epi*-AZA1. LC-MS chromatograms prior to and following treatment with periodate. MS and NMR spectra showing incorporation of deuterium after storage in CH_3OD and CD_3OD. Kinetics of deuterium exchange (in, in CH_3OD, then out again, in PBS). Mass spectra showing stability of deuterated AZA1 during storage in buffer. LC-MS chromatograms showing formation of AZA3 methyl ketals. HPLC-FLD chromatograms following ADAM derivatization. Kinetic data on epimerization of 37-*epi*-AZA1. NMR spectra of: AZA1 in CD_3OD, CD_3OH, and d_6-DMSO; 37-*epi*-AZA1 in CD_3OD and CD_3OH; and AZA2 in CD_3OD. High resolution

MS/MS spectra of AZA1 and deuterated AZA2. This information is available free of charge via the Internet at http://pubs.acs.org/.

ABBREVIATIONS

AZA, azaspiracid; COSY, correlation spectroscopy; DEPT135, distortionless enhancement by polarisation transfer (135°); EC_{50}, half maximal effective concentration; EU, European Union; ESI, electrospray ionization; FA, formic acid; HMBC, heteronuclear multiple-bond correlation; HSQC, heteronuclear single quantum correlation; NoE, nuclear overhauser effect; NOESY, ROESY, rotating frame NOE spectroscopy; PBS, phosphate-buffered saline; Rel. Pot., relative potency; SELROESY, selected ROESY; SELTOCSY, selected TOCSY; SIM, selected ion monitoring; SRM, selected reaction monitoring; TEA, triethylamine; TOCSY, total correlation spectroscopy.

REFERENCES

(1) Tillmann, U., Elbrächter, M., Krock, B., John, U., and Cembella, A. D. (2009) *Azadinium spinosum* gen. et sp. nov. (Dinophyceae) identified as a primary producer of azaspiracid toxins. *Eur. J. Phycol. 44*, 63–79.

(2) Krock, B., Tillmann, U., Voß, D., Koch, B. P., Salas, R., Witt, M., Potvin, É., and Jeong, H. J. (2012) New azaspiracids in *Amphidomataceae* (Dinophyceae). *Toxicon 60*, 830–839.

(3) Satake, M., Ofuji, K., Naoki, H., James, K. J., Furey, A., McMahon, T., Silke, J., and Yasumoto, T. (1998) Azaspiracid, a new marine toxin having unique spiro ring assemblies, isolated from Irish mussels, *Mytilus edulis*. *J. Am. Chem. Soc. 120*, 9967–9968.

(4) Krock, B., Tillmann, U., John, U., and Cembella, A. D. (2009) Characterization of azaspiracids in plankton size-fractions and isolation of an azaspiracid-producing dinoflagellate from the North Sea. *Harmful Algae 8*, 254–263.

(5) Salas, R., Tillmann, U., John, U., Kilcoyne, J., Burson, A., Cantwell, C., Hess, P., Jauffrais, T., and Silke, J. (2011) The role of *Azadinium spinosum* (Dinophyceae) in the production of azaspiracid shellfish poisoning in mussels. *Harmful Algae 10*, 774–783.

(6) McCarron, P., Kilcoyne, J., Miles, C. O., and Hess, P. (2009) Formation of azaspiracids-3, -4, -6, and -9 via decarboxylation of carboxyazaspiracid metabolites from shellfish. *J. Agric. Food Chem. 57*, 160–169.

(7) Rehmann, N., Hess, P., and Quilliam, M. A. (2008) Discovery of new analogs of the marine biotoxin azaspiracid in blue mussels (*Mytilus edulis*) by ultra-performance liquid chromatography/tandem mass spectrometry. *Rapid Commun. Mass Spectrom. 22*, 549–558.

(8) Anon. (2011) Commission Regulation (EU) No 15/2011 of 10th January 2011 amending Regulation (EC) No 2074/2005 as regards recognised testing methods for detecting marine biotoxins in live bivalve molluscs. L6/3-6. http://eurlex.europa.eu/LexUriServ/LexUriServ.do?uri=OJ:L:2011:006:0003:0006:EN:PDF

(9) Ofuji, K., Satake, M., McMahon, T., Silke, J., James, K. J., Naoki, H., Oshima, Y., and Yasumoto, T. (1999) Two analogues of azaspiracid isolated from mussels, *Mytilus edulis*, involved in human intoxications in Ireland. *Nat. Toxins 7*, 99–102.

(10) Ofuji, K., Satake, M., McMahon, T., James, K. J., Naoki, H., Oshima, Y., and Yasumoto, T. (2001) Structures of azaspiracid analogs, azaspiracid-4 and azaspiracid-5, causative toxins of azaspiracid poisoning in Europe. *Biosci. Biotechnol. Biochem. 65*, 740–742.

(11) Kilcoyne, J., Keogh, A., Clancy, G., LeBlanc, P., Burton, I., Quilliam, M. A., Hess, P., and Miles, C. O. (2012) Improved isolation procedure for azaspiracids from shellfish, structural elucidation of azaspiracid-6, and stability studies. *J. Agric. Food Chem. 60*, 2447–2455.

(12) Twiner, M. J., Hess, P., and Doucette, G. (2014) Azaspiracids: toxicology, pharmacology, and risk assessment, in *Seafood and Freshwater Toxins, 3rd Edition* (Botana, L. M., Ed.) in press, CRC Press, Boca Raton, FL.

(13) Twiner, M. J., Rehmann, N., Hess, P., and Doucette, G. J. (2008) Azaspiracid shellfish poisoning: a review on the chemistry, ecology, and toxicology with an emphasis on human health impacts. *Mar. Drugs 6*, 39–72.

(14) McMahon, T., and Silke, J. (1996) Winter toxicity of unknown aetiology in mussels. *Harmful Algae News 14*.

(15) Ito, E., Satake, M., Ofuji, K., Kurita, N., McMahon, T., James, K., and Yasumoto, T. (2000) Multiple organ damage caused by a new toxin azaspiracid, isolated from mussels produced in Ireland. *Toxicon 38*, 917–930.
(16) Satake, M., Ofuji, K., James, K. J., Furey, A., and Yasumoto, T. (1998) New toxic event caused by Irish mussels, in *Harmful Algae* (Reguera, B., Blanco, J., Fernandez, M. L., Wyatt, T., Eds.) pp 468–469, Xunta de Galicia and Intergovernmental Oceanographic Commission of UNESCO, Santiago de Compostela, Spain.
(17) McMahon, T., and Silke, J. (1998) Re-occurence of winter toxicity. *Harmful algae News 17*, 12.
(18) Aasen, J. A. B., Espenes, A., Hess, P., and Aune, T. (2010) Sub-lethal dosing of azaspiracid-1 in female NMRI mice. *Toxicon 56*, 1419–1425.
(19) Aasen, J. A. B., Espenes, A., Miles, C. O., Samdal, I. A., Hess, P., and Aune, T. (2011) Combined oral toxicity of azaspiracid-1 and yessotoxin in female NMRI mice. *Toxicon 57*, 909–917.
(20) Aune, T., Espenes, A., Aasen, J. A. B., Quilliam, M. A., Hess, P., and Larsen, S. (2012) Study of possible combined toxic effects of azaspiracid-1 and okadaic acid in mice via the oral route. *Toxicon 60*, 895–906.
(21) Twiner, M. J., Hanagriff, J. C., Butler, S., Madhkoor, A. K., and Doucette, G. J. (2012) Induction of apoptosis pathways in several cell lines following exposure to the marine algal toxin azaspiracid-1. *Chem. Res. Toxicol. 25*, 1493–1501.
(22) Twiner, M. J., Hess, P., Bottein Dechraoui, M. Y., McMahon, T., Samons, M. S., Satake, M., Yasumoto, T., Ramsdell, J. S., and Doucette, G. J. (2005) Cytotoxic and cytoskeletal effects of azaspiracid-1 on mammalian cell lines. *Toxicon 45*, 891–900.
(23) Twiner, M. J., Ryan, J. C., Morey, J. S., Smith, K. J., Hammad, S. M., Van Dolah, F. M., Hess, P., McMahon, T., Satake, M., Yasumoto, T., and Doucette, G. J. (2008) Transcriptional profiling and inhibition of cholesterol biosynthesis in human T lymphocyte cells by the marine toxin azaspiracid. *Genomics 91*, 289–300.
(24) Vale, C., Nicolaou, K. C., Frederick, M. O., Gomez-Limia, B., Alfonso, A., Vieytes, M. R., and Botana, L. M. (2007) Effects of azaspiracid-1, a potent cytotoxic agent, on primary neuronal cultures. A structure-activity relationship study. *J. Med. Chem. 50*, 356–363.
(25) Kulagina, N. V., Twiner, M. J., Hess, P., McMahon, T., Satake, M., Yasumoto, T., Ramsdell, J. S., Doucette, G. J., Ma, W., and O'Shaughnessy, T. J. (2006) Azaspiracid-1 inhibits bioelectrical activity of spinal cord neuronal networks. *Toxicon 47*, 766–773.
(26) Twiner, M. J., El-Ladki, R., Kilcoyne, J., and Doucette, G. J. (2012) Comparative effects of the marine algal toxins azaspiracid- 1, -2, and -3 on Jurkat T lymphocyte cells. *Chem. Res. Toxicol. 25*, 747–754.
(27) Twiner, M. J., Doucette, G. J., Rasky, A., Huang, P. X., Roth, B. L., and Sanguinetti, M. C. (2012) The marine algal toxin azaspiracid is an open state blocker of hERG potassium channels. *Chem. Res. Toxicol. 25*, 1975–1984.
(28) Quilliam, M. A.; Reeves, K.; MacKinnon, S.; Craft, C.; Whyte, H.; Walter, J.; Stobo, L.; Gallacher, S. (2006) Preparation of reference materials for azaspiracids, in *Proceedings of the 5th International Conference of Molluscan Shellfish Safety* (Deegan, B., Butler, C., Cusack, C., Henshilwood, K., Hess, P., Keaveney, S., McMahon, T., O'Cinneide, M., and Silke, J., Eds.) pp 111–115, Marine Institute, Galway, Ireland.
(29) Hess, P., McCarron, P., Rehmann, N., McMahon, T., Ryan, G., Ryan, M., Twiner, M. J., Doucette, G. J., Satake, M., Ito, E., and Yasumoto, T. (2007)

Isolation and purification of azaspiracids from naturally contaminated materials, and evaluation of their toxicological effects—final project report ASTOX (ST/02/02). *Marine Institute—Marine Environment & Health Series—No. 28, ISSN: 1649-0053. http://www.marine.ie/NR/rdonlyres/2B06863D-3366-47CD-9ABB-B3302629FE46/0/ASTOX.pdf.*

(30) McCarron, P., Emteborg, H., and Hess, P. (2007) Freeze-drying for the stabilisation of shellfish toxins in mussel tissue (*Mytilus edulis*) RMs. *Anal. Bioanal. Chem*. *387*, 2475–86.

(31) McCarron, P., Kotterman, M., De Boer, J., Rehmann, N., and Hess, P. (2007) Feasibility of irradiation as a stabilisation technique in the preparation of tissue RMs for a range of shellfish toxins. *Anal. Bioanal. Chem. 387*, 2487–93.

(32) Perez, R., Rehmann, N., Crain, S., LeBlanc, P., Craft, C., MacKinnon, S., Reeves, K., Burton, I., Walter, J. A., Hess, P., Quilliam, M. A., and Melanson, J. (2010) The preparation of certified calibration solutions for azaspiracid-1, -2, and -3, potent marine biotoxins found in shellfish. *Anal. Bioanal. Chem. 398*, 2243–2252.

(33) McCarron, P., Giddings, S. D., Reeves, K., and Quilliam, M. A. (2011) CRM-AZA-Mus-200603 CRMP Technical report, in *CRMP Technical Report CRM-AZA-Mus-200603*, 2011.

(34) Quilliam, M. A., Hess, P., Dell'Aversano, C., Koe, W., Samson, R., Van Egmond, H., Gilbert, J., and Sabino, M. (2001) Mycotoxins and phycotoxins in perspective at the turn of the century, in *Proceedings of the Xth international IUPAC symposium on mycotoxins and phycotoxins* (deKoe, W. J., Samson, R. A., van Egmond, H. P., Gilbert, J., and Sabino, M., Eds.) pp383–391, deKoe, W. J., The Netherlands.

(35) McNabb, P., Selwood, A. I., and Holland, P. T. (2005) Multiresidue method for determination of algal toxins in shellfish: single-laboratory validation and interlaboratory study. *AOAC Int. 88*, 761–772.

(36) Kilcoyne, J., and Fux, E. (2010) Strategies for the elimination of matrix effects in the liquid chromatography tandem mass spectrometry analysis of the lipophilic toxins okadaic acid and azaspiracid-1 in molluscan shellfish. *J. Chromatogr. A 1217*, 7123–7130.

(37) Gerssen, A., Mulder, P. J., McElhinney, M. A., and De Boer, J. (2009) Liquid chromatography–tandem mass spectrometry method for the detection of marine lipophilic toxins under alkaline conditions. *J. Chromatogr. A 1216*, 1421–1430.

(38) McCarron, P., Giddings, S. D., and Quilliam, M. A. (2011) A mussel tissue certified reference material for multiple phycotoxins. Part 2: liquid chromatography–mass spectrometry, sample extraction and quantitation procedures. *Anal. Bioanal. Chem. 400*, 835–846.

(39) Alfonso, C., Rehmann, N., Hess, P., Alfonso, A., Wandscheer, C., Abuin, M., Vale, C., Otero, P., Vieytes, M., and Botana, L. M. (2008) Evaluation of various pH and temperature conditions on the stability of azaspiracids and their importance in preparative isolation and toxicological studies. *Anal. Chem. 80*, 9672–9680.

(40) Lamberty, A., Schimmel, H., and Pauwels, J. (1998) The study of the stability of reference materials by isochronous measurements. *J. Anal. Chem. 360*, 359–361.

(41) Burton, I., Quilliam, M. A., and Walter, J. A. (2005) Quantitative ^{1}H NMR with external standards: use in preparation of calibration solutions for algal toxins and other natural products. *Anal. Chem. 77*, 3123–3131.

(42) McCarron, P., Giddings, S. D., Miles, C. O., and Quilliam, M. A. (2011) Derivatization of azaspiracid biotoxins for analysis by liquid chromatography with fluorescence detection. *J. Chromatogr. A 1218*, 8089–8096.
(43) Nicolaou, K. C., Li, Y. W., Uesaka, N., Koftis, T. V., Vyskocil, S., Ling, T. T., Govindasamy, M., Qian, W., Bernal, F., and Chen, D. Y. K. (2003) Total synthesis of the proposed azaspiracid-1 structure, part 1: construction of the enantiomerically pure C1-C20, C21-C27, and C28-C40 fragments. *Angew. Chem. Int. Edit. 42*, 3643–3648.
(44) Nicolaou, K. C., Chen, D. Y. K., Li, Y. W., Qian, W. Y., Ling, T. T., Vyskocil, S., Koftis, T. V., Govindasamy, M., and Uesaka, N. (2003) Total synthesis of the proposed azaspiracid-1 structure, part 2: coupling of the C1-C20, C21-C27, and C28-C40 fragments and completion of the synthesis. *Angew. Chem. Int. Edit. 42*, 3649–3653.
(45) Nicolaou, K. C., Frederick, M. O., Petrovic, G., Cole, K. P., and Loizidou, E. Z. (2006) Total synthesis and confirmation of the revised structures of azaspiracid-2 and azaspiracid-3. *Angew. Chem. Int. Edit. 45*, 2609–2615.
(46) Larsen, K., Petersen, D., Wilkins, A. L., Samdal, I. A., Sandvik, M., Rundberget, T., Goldstone, D., Arcus, V., Hovgaard, P., Rise, F., Rehmann, N., Hess, P., and Miles, C. O. (2007) Clarification of the C-35 stereochemistries of dinophysistoxin-1 and dinophysistoxin-2, and its consequences for binding to protein phosphatase. *Chem. Res. Toxicol. 20*, 868–875.
(47) Vilariño, N., Nicolaou, K., Frederick, M. O., Cagide, E., Ares, I. R., and Louzao, M. C. (2006) Cell growth inhibition and actin cytoskeleton disorganization induced by azaspiracid-1 structure-activity studies. *Chem. Res. Toxicol. 19*, 1459–1466.
(48) Vilariño, N., Nicolaou, K. C., Frederick, M. O., Vieytes, M. R., and Botana, L. M. (2007) Irreversible cytoskeletal disarrangement is independent of caspase activation during *in vitro* azaspiracid toxicity in human neuroblastoma cells. *Biochem. Pharmacol. 74*, 327–335.

Table 1. Half-life (days)[a] for 37-*epi*-AZA1, AZA2 and AZA3 in aqueous acetonitrile at 40 °C

Treatment	37-*epi*-AZA1	37-*epi*-AZA2	37-*epi*-AZA3
0.1% Formic acid	7.5	7.0	2.1
Neutral	11	11	4.5
0.1 % TEA	38	32	28

[a]From LC-MS data fitted to exponential decay curve with 16% epimer at equilibrium, using SigmaPlot 12.0.

Table 2. NMR assignments for AZA2 and 37-*epi*-AZA2 from a partially epimerized sample in CD_3OD

	AZA2		37-*epi*-AZA2	
Atom	^{13}C	^{1}H	^{13}C	^{1}H
1	181.3		n.r.	
2	38.3	2.24, 2.24	n.r.	n.r.
3	30.3	2.32, 2.32	n.r.	n.r.
4	133.5	5.73	n.r.	n.r.
5	131.2	5.41	n.r.	n.r.
6	72.7	4.72	n.r.	n.r.
7	123.1	5.34	n.r.	n.r.
8	131.0		n.r.	
9	40.4	1.98, 2.43	n.r.	n.r.
10	107.5		n.r.	
11	37.4	1.97, 2.16	n.r.	n.r.
12	33.2	1.66, 2.33	n.r.	n.r.
13	111.3		n.r.	
14	31.0	2.01	n.r.	2.01
15	32.6	1.74, 1.84	n.r.	1.75, 1.82
16	78.2	3.89	78.1	3.91
17	73.3	4.20	73.0	4.17
18	37.4	2.01, 2.01	n.r.	2.00, 2.06
19	79.2	4.43	n.r.	4.43
20	77.0	3.82	77.0	3.50
21	100.1		99.8	
22	36.6	2.13	35.9	2.30
23	38.5	1.43, 1.43	n.r.	1.41, 1.41
24	42.2	1.36	n.r.	1.35
25	79.7	3.97	79.8	3.88
26	148.2		148.1	
27	49.5	2.23, 2.41	49.2	2.14, 2.37
28	98.5		n.r.	
29	44.3	1.35, 2.03	44.1	1.32, 2.00
30	26.5	2.24	n.r.	2.26
31	35.5	1.51, 1.82	n.r.	1.50, 1.78
32	72.8	4.33	72.7	4.24
33	81.0	3.97	79.0	3.81
34	75.0	4.95	75.4	4.82
35	42.1	2.34[a], 2.56		n.r., 2.13
36	96.5		96.6	
37	36.2	1.93	37.3	n.r.
38	38.3	1.26, 1.65	38.9	1.45, 1.73
39	30.1	1.82	n.r.	1.84
40	46.5	2.75, 2.80	47.9	2.62, 2.67
8-Me	23.0	1.69	n.r.	n.r.
14-Me	16.7	0.94	n.r.	0.94
22-Me	16.4	0.91	16.5	0.90

24-Me	18.1	0.83	18.1	0.82
26=CH2	116.6	5.16, 5.33	115.7	5.13, 5.28
30-Me	23.6	0.95	23.9	0.94
37-Me	15.6	0.95	15.9	1.06
39-Me	18.8	0.93	19.3	0.88

[a]Exchanges deuterium

n.r., not resolved from AZA2 signals

Table 3. NMR assignments for AZA1 and 37-*epi*-AZA1

	AZA1 in CD_3OD		AZA1 in CD_3OH		AZA1 in CD_3OD + 0.5% CD_3CO_2D[a]		AZA1 in d_6-DMSO		37-*epi*-AZA1 in CD_3OD	
Atom	^{13}C	^{1}H	^{13}C	^{1}H	^{13}C	^{1}H	^{13}C	^{1}H	^{13}C	^{1}H
1	181.2		180.6		180.3		n.r.	n.r.	181.3	
2	38.1	2.25, 2.25	37.6	2.25, 2.25	37.4	2.31, 2.31	n.r.	n.r.	38.4	2.25, 2.25
3	30.2	2.33, 2.33	29.9	2.33, 2.33	30.3	2.33, 2.33	27.3	2.21	30.3	2.33, 2.33
4	133.7	5.75	133.4	5.74	133.8	5.74	128.1	5.63	133.7	5.75
5	130.7	5.44	130.6	5.43	131.8	5.46	129.5	5.39	130.7	5.44
6	72.5	4.79	72.3	4.78	73.2	4.81	70.2	4.71	72.5	4.80
7	129.4	5.63	129.3	5.63	130.1	5.65	122.4	5.61	129.4	5.64
8	123.2	5.73	123.1	5.72	124.1	5.76	122.4	5.71	123.3	5.73
9	35.7	2.12, 2.46	35.6	2.12, 2.47	36.5	2.15, 2.49	34.4	2.03, 2.43	35.8	2.12, 2.48
10	107.2		107.1		107.9		105.0		107.3	
11	37.5	1.97, 2.14	37.4	1.95, 2.13	38.3	1.97, 2.16	36.2	1.89, 2.02	37.6	1.95, 2.14
12	33.2	1.66, 2.33	33.1	1.65, 2.32	33.9	1.68, 2.33	31.9	1.54, 2.19	33.3	1.65, 2.33
13	111.3		111.2		112.1		109.2		111.4	
14	31.0	2.02	80.8	2.01	31.7	2.02	29.3	1.89	31.1	2.03
15	32.6	1.76, 1.85	32.5	1.75, 1.84	33.4	1.77, 1.85	31.3	1.60, 1.71	32.7	1.76, 1.83
16	78.2	3.88	78.1	3.88	79.1	3.89	75.6	3.84	78.1	3.91
17	73.3	4.23	73.2	4.22	74.2	4.25	71.1	4.05	73.0	4.20
18	37.3	1.99, 2.01	37.1	1.95, 1.99	37.8	2.00, 2.01	37.7	1.86, 1.98	39.0	2.00, 2.07
19	79.2	4.43	79.1	4.42	79.9	4.44	77.7	4.26	79.2	4.43
20	76.9	3.86	76.8	3.88	77.6	3.94	74.8	3.25	77.0	3.50
21	100.2		100.2		101.1		97.8		99.9	
22	36.6	2.12	36.6	2.09	37.6	2.09	34.3	2.17	35.9	2.30
23	38.3	1.43, 1.43	38.1	1.42, 1.42	38.9	1.44, 1.44	37.3	1.31, 1.31	38.6	1.42, 1.42
24	42.3	1.35	42.1	1.34	43.1	1.35	40.4	1.22	42.2	1.36
25	79.6	3.98	79.5	3.97	80.4	4.00	77.5	3.81	79.9	3.87
26	148.3		148.2		149.1		146.7		148.1	
27	49.5	2.24, 2.42	49.6	2.23, 2.41	50.4	2.26, 2.43	47.5	2.04, 2.25	49.0	2.14, 2.37

28	98.6		98.5		99.5		95.9		98.3	
29	44.3	1.36, 2.03	44.1	1.35, 2.03	44.9	1.37, 2.05	43.4	1.20, 1.9	44.6	1.32, 2.00
30	26.4	2.23	26.3	2.22	27.2	2.23	24.8	2.17	26.7	2.26
31	35.4	1.52, 1.83	35.2	1.51, 1.82	36.1	1.54, 1.84	34.3	1.33, 1.71	35.5	1.50, 1.78
32	72.8	4.35	72.7	4.34	73.6	4.38	70.8	4.13	72.2	4.24
33	81.2	4.01	81.2	4.02	82.3	4.08	76.9	3.61	78.8	3.81
34	74.9	4.98	74.8	4.98	75.6	5.02	73.7	4.68	75.4	4.83
35	41.9	2.41, 2.59	47.7	2.43, 2.59	42.5	2.50[c]	41.7	1.76, 2.21	45.1	2.11[b]
36	96.6		96.5		97.4		93.9		96.8	
37	36.0	1.95	35.8		36.4	1.99	36.4	1.58	39.1	1.78
38	38.0	1.28, 1.67	37.8	1.28, 1.66	38.4	1.31, 1.70	38.8	1.00, 1.45	36.8	1.45, 1.73
39	29.8	1.85	29.6	1.85	30.2	1.89	30.4	1.53	25.0	1.84
40	46.4	2.79, 2.84	46.3	2.79, 2.86	46.9	2.84, 2.91	46.3	2.33, 2.38	47.8	2.62, 2.67
14-Me	16.6	0.95	16.5	0.94	17.4	0.95	15.9	0.86	16.7	0.95
22-Me	16.4	0.91	16.3	0.90	17.2	0.91	16.3	0.789	16.6	0.90
24-Me	18.1	0.84	17.9	0.83	18.8	0.84	17.5	0.738	18.1	0.82
26=CH2	116.8	5.16, 5.34	116.8	5.16, 5.33	117.2	5.18, 5.36	113.4	4.96, 5.11	115.5	5.13, 5.28
30-Me	23.5	0.95	23.4	0.95	24.3	0.96	23.3	0.84	23.9	0.94
37-Me	15.5	0.96	15.4	0.96	16.2	0.98	15.7	0.75	15.8	1.06
39-Me	18.6	0.94	18.4	0.94	19.3	0.95	19.0	0.76	19.3	0.88

[a]NMR data from Satake et al.[3]; solvent composition, personal communication from M. Satake.
[b]One of the H-35 signals not identified due to exchange
n.r., not resolved from AZA1 signals

Table 4. Relative molar response factors (with standard deviation of the last significant figure in parenthesis) of 37-*epi*-AZA1 in relation to AZA1 (AZA1(area/concentration)/37-*epi*-AZA1(area/concentration))[a]

	Neutral		Acidic	
MS mode (ion/transition)	Gradient[b]	Isocratic[c]	Gradient[d]	Isocratic[e]
SIM (842.5)		0.94 (3)		0.93 (3)
SRM (842→824)	0.912 (4)	0.883 (3)	0.860 (4)	0.882 (4)
SRM (842→806)	1.016 (7)	0.995 (5)	0.977 (5)	0.971 (3)
SRM (842→672)	0.968 (3)	0.920 (3)	0.913 (5)	0.912 (5)
SRM (842→654)	0.588 (4)	0.580 (2)	0.554 (3)	0.554 (1)
SRM (842→462)	0.801 (4)	0.763 (3)	0.745 (4)	0.746 (2)
SRM (842→362)	1.106 (6)	1.105 (4)	1.091 (7)	1.097 (2)

[a]Determined by SIM and SRM LC-MS experiments using gradient and isocratic LC elution with neutral and acidic mobile phases. Propagated standard deviations (of the last significant figure) from LC-MS/MS analyses are shown in parentheses. [b]Method C(i). [c]Method C(ii). [d]Method C(iii). [e]Method C(iv).

Table 5. Calculated EC_{50} values (nM) with 95% confidence intervals (CI) and relative potencies (Rel. Pot.) for AZA analogues based on T lymphocyte cytotoxicity

AZA analogue	24 h		48 h		72 h		Mean EC_{50}	Rel. Pot.
	EC_{50}	95% CI	EC_{50}	95% CI	EC_{50}	95% CI		
AZA1	0.96	0.19–4.9	1.10	0.46–2.5	1.3	0.59–3.0	1.1	1.0
37-*epi*-AZA1	0.15	0.053–0.41	0.27	0.13–0.53	0.24	0.12–0.48	0.22	5.1

Table 6. Proportions of 37-*epi*-AZA1 and AZA1 following exposure to the Jurkat T lymphocyte cell assay (37 °C) and in the absence of cells in aqueous acetonitrile at 40 °C (n = 3).

	Jurkat T lymphocyte cells (37-*epi*-AZA1)		Jurkat T lymphocyte cells (AZA1)		Aqueous Acetonitrile	
Time	% 37-*epi*-AZA1	% AZA1	% 37-*epi*-AZA1	% AZA1	% 37-*epi*-AZA1	% AZA1
0	94 ± 1	6 ± 1	4 ± 1	96 ± 1	96 ± 1	4 ± 1
24	27 ± 5	73 ± 1	11 ± 1	89 ± 1	89 ± 1	11 ± 1
48	14 ± 2	86 ± 1	12 ± 1	88 ± 1	86 ± 1	14 ± 1
72	12 ± 1	88 ± 1	12 ± 1	88 ± 1	76 ± 1	24 ± 1